Sensors, Sampling, and Simulation for Process Control
Edited by: Brian G. Thomas, James A. Yurko, and Lifeng Zhang
TMS (The Minerals, Metals & Materials Society), 2011
Annual Meeting, San Diego, CA, Feb. 27 - Mar. 3, 2011.

IMPLEMENTATION OF TEMPERATURE AND STRAIN MICRO-SENSORS INTO A CASTING MOLD SURFACE

B.G. Thomas and M.K. Okelman

Department of Mechanical Science and Engineering,
University of Illinois at Urbana-Champaign; 1206 West Green Street, Urbana, IL 61801

Keywords: Fiber Bragg Grating, Thin-film thermocouples, Embedded sensors, Measurement, Continuous casting, Coatings, Electroplating

Abstract

Microfabricated thin-film thermocouples (TFTCs) and Fiber Bragg Grating (FBG) sensors can be embedded in the coating layers of the mold during electroplating to measure temperature, heat flux, and strain during continuous casting. Embedding sensors within 1mm near the surface has the advantages of sensitive real-time monitoring of thermal behavior without damping by the copper mold, and protection from the hostile environment. A method to embed TFTCs and FBG optical fibers in a coating layer was developed, implemented and tested. The signal output by FBG sensors embedded in a nickel coating layer on a copper mold has been investigated and can be predicted with simple equations. These sensors are able to monitor both temperature and strain in real time during casting operation with high resolution.

Introduction

Many problems in continuous casting of steel and other processes arise during initial solidification near the meniscus where molten metal first touches the mold. These include surface defects in the final product as well as cracks in the mold surface due to thermal stress. Understanding the underlying phenomena and controlling them requires both advanced modeling and measurements. Sensors are limited to indirect measurements, because the mold surface and beyond is an extremely hostile environment and sensors there would interfere with the process. In current industrial practice, several horizontal rows of thermocouples are embedded into each mold wall, keeping 7 to 20 mm away from the hot face, due to safety considerations [1]. Their temperature signals are interpreted by systems installed in most casters to control mold level control [1], to detect and prevent sticker breakouts [2], and to monitor steel quality [3]. While they are very useful, these systems are limited by the slow response time of the thermocouples, which are dampened by the thick copper mold layer between them and the solidifying steel, so they cannot fully capture the rapid thermal events that occur at the meniscus [4, 5]. Moreover, problems related to thermal distortion of the mold, and thermal cracks cannot be detected, owing to the lack of robust thermal strain sensors.

Microfabricated thin-film thermocouples (TFTCs) and / or Fiber Bragg Grating (FBG) sensors can be embedded in the nickel coating layer that is electroplated onto many continuous-casting molds and then used to measure temperature, heat flux, and thermal strain within 1 mm of the meniscus. This cost-effective method would enable sensitive real-time monitoring of critical thermal and mechanical behavior with fast response time, and protection from the hostile environment. With the ability to place many sensors within close proximity of one another, embedded sensors could enable more accurate prediction of liquid level and its transient

fluctuations. More sensitive online monitoring of mold temperature variations would extend their usefulness, providing additional insights into casting phenomena, thereby enabling detection of the formation of defects such as longitudinal cracks, by better distinguishing their distinctive temperature-history "signatures" [5].

Implementing these advantageous micro-sensors requires a robust attachment method that 1) provides a secure bond between the sensor and the copper with no gaps, 2) enables the sensor to survive the acid pretreatment and electroplating processes, and 3) allows it to provide accurate measurements during operation. This paper presents the design, installation, and interpretation of micro-sensors in commercial molds for continuous casting of steel. Equations are developed to interpret the signals from embedded FBG sensors as functions of temperature and strain. The final system proposed aims 1) to revolutionize online thermal monitoring of industrial continuous casting molds and 2) to create a new research tool to investigate meniscus behavior so that defect formation can be better understood.

The design is presented in Fig. 1, for the example of a TFTC sensor strip. In addition to their expense, these rectangular cross-section sensors were found to be susceptible to gap formation during plating, which could cause catastrophic temperature increases during operation [6]. Their implementation is still feasible using a robust conductive silver paste, as discussed elsewhere [6]. This paper focuses on FBG sensors.

The first step is to embed the fiber containing the sensor(s) into the coating layer during electroplating of the mold. The optical fiber consists of a 9 µm diameter core, protected with a 125 µm thick layer of thermoset polyimide, which can survive the entire temperature range of mold operation up to 500°C [7]. The total fiber diameter of 155µm easily fits inside a typical 300 - 400 µm thick nickel coating layer. Each FBG sensing region consists of several grating layers that are optically etched into the fiber in order to amplify and reflect back light of a particular frequency. After plating, the sensor fiber extends from to the top of the mold, allowing easy extraction of the sensor signals to a computer, such as by attachment to a miniature circuit box for wireless transmission to a computer located elsewhere.

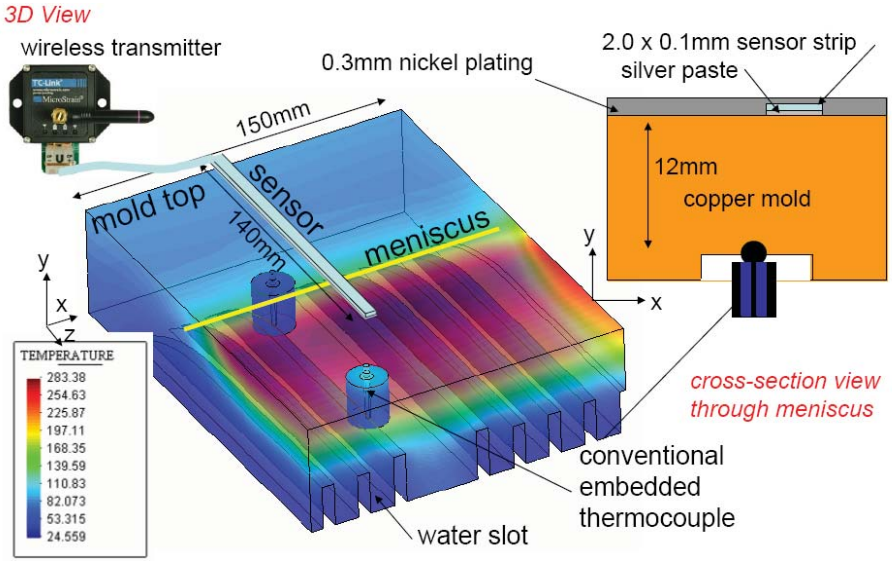

Figure 1. Sensor embedded in Ni coating layer of continuous casting mold (temperature in °C)

Testing was conducted to embed optical fibers into the nickel coating layer of continuous casting mold samples using the commercial electroplating process for continuous casting molds at a commercial mold plating facility in Benton Harbor, MI. Pretreatment involved immersion in dilute acid solution, followed by electroplating in nickel sulfamate for several hours. Cylindrical fibers always produced sound plating, for both conducting and insulating fiber materials. Sound plating was found even when several fibers were very close together, as seen in Fig. 2. Such close spacing can enable high spatial resolution.

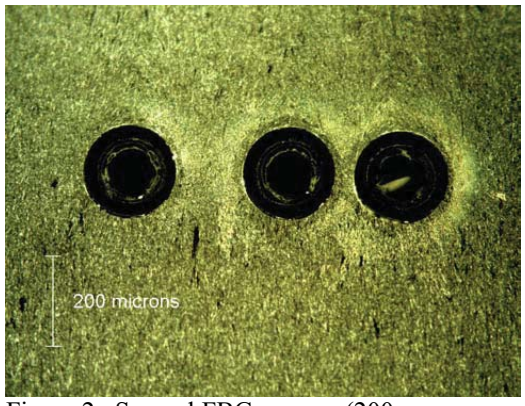

Figure 2. Several FBG sensors (200 µm diameter, plastic coated optical fibers) after electroplating with nickel

Close proximity to the substrate also produced sound plating. Further details on the electroplating trials are reported elsewhere [8].

Trials were conducted on both embedded FBG fibers and on 316-stainless steel tubes containing the fibers. The latter are pictured in Fig. 3. A closeup of the fiber exiting the tube near the top of the mold is shown in Fig. 4. Larger tubes (OD 330 µm, ID 178 µm) contained the 155 µm diameter plastic-coated fibers, while smaller tubes (OD 254 µm, ID 127 µm) housed bare optical glass fibers.

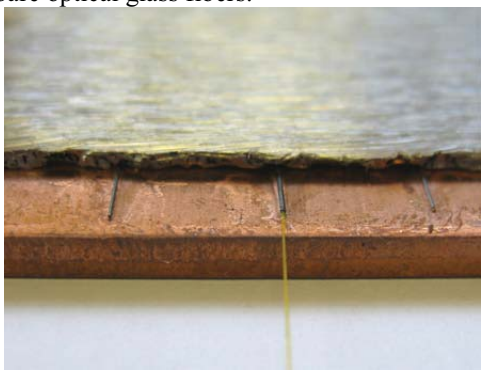

Figure 3. Stainless steel tubes embedded in coating layer

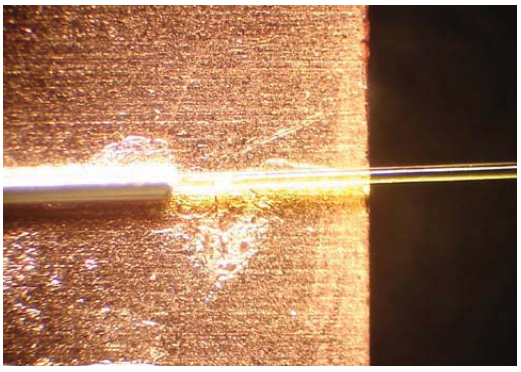

Figure 4. Closeup of polyimide-coated fiber with FBG sensors inserted into a steel tube

Having demonstrated that both cylindrical optical fibers and steel tubes containing free-moving fibers can be embedded soundly into the mold coating, heating and cooling tests were conducted on the final system to demonstrate the ability of the sensors to measure temperature and strain. The fiber was a transmission-type FBG sensor with center wavelength 1543.30 nm (provided by O/E Land Inc.). A second fiber of just the bare-glass core was damaged during handling, which is a difficulty to address for commercial operation. Specifically, the fibers extending from the mold need to be encased in temporary protective material during plating, and the fragile junction where they attach to the transmission box at the top of the mold needs to be protected during operation.

Interpretation of Fiber-Bragg-Grating Sensor Signals

The interactions between the sensor and substrate are complex, so interpretation of the signals from the FBG sensors into temperature or strain measurements is not simple. Each FBG sensor measures a Bragg wavelength shift according to the length fiber length, with changes with both temperature and mechanical strain. The signal output is potentially a combination of four quantities (three principle strains and temperature) [9]. It is possible to calibrate a FBG sensor (or FBG sensor system containing more than one sensor) for a given load, but the results would only be valid under conditions that produce a nearly identical temperature and strain as those used during calibration. Instead, for structurally embedded FBG sensor temperature measurement systems it is better to determine the optical properties of the FBG sensor as a function of temperature and wavelength [9] and use them together with the FBG sensor's strain-based properties to predict the temperature.

The signal output by the FBG sensor corresponds to the temperature and strain at the FBG sensor, not to the substrate, as a sensor embedded inside the substrate disturbs the strain and temperature field. The signal output by the FBG sensor (the "temperature" and "strain" at the sensor) must be related to the temperature and strain in the host material. This analysis has been conducted for both bare and coated fiber optic sensors [6,10]. The results show that some of the strain components inside the sensor may differ if the sensor is bare or coated. Furthermore, the difference depends on the thickness and properties of the coating.

As inferred from above, when a strain is applied to a FBG sensor its grating spectral response, or Bragg wavelength, is changed (i.e. the Bragg wavelength is dependent on both temperature and strain). Assuming that the bond between the fiber and the substrate is strong (i.e. the "temperature" and "strain" at the sensor is equal to the temperature and strain of the substrate), the total Bragg wavelength shift for an embedded FBG sensor has two components:

$$\Delta\lambda_{total} = \Delta\lambda_{temperature} + \Delta\lambda_{strain} \tag{5}$$

The thermal effect component ($\Delta\lambda_{temperature}$) is related to the change in index of refraction:

$$\Delta\lambda_{temperature} = \lambda_{CW}\left(\alpha_f + \frac{1}{n_0}\frac{dn_0}{dT}\right)\left(T - T_0\right) \tag{6}$$

where λ_{CW} is the Bragg center wavelength of the FBG sensor (1543.30 nm for the embedded FBG sensor, 1541.04 nm for the free-floating FBG sensor), α_f is the coefficient of thermal expansion (CTE) of the fiber (i.e. silica), n_0 is the index of refraction, dn_0/dT is the thermo-optic coefficient, T_0 is defined as the temperature at the first measurement of the Bragg wavelength, λ_0, during calibration and T is the temperature corresponding to any of the Bragg wavelength measurements.

The strain component ($\Delta\lambda_{strain}$) due to the physical elongation of the sensor, as well as the change in refractive index due to photoelastic effects, is given by:

$$\Delta\lambda_{strain} = \lambda_{CW}\left(1 - p_e\right)\left(\varepsilon - \alpha_f\left(T - T_0\right)\right) \tag{7}$$

where ε is the mechanical strain and p_e is the photoelastic coefficient given by:

$$p_e = \left(\frac{n_0^2}{2}\right)\left[p_{12} - \nu\left(p_{11} + p_{12}\right)\right] \tag{8}$$

where ν is the Poisson's ratio of the fiber (i.e. silica) and p_{11} and p_{12} are Pockel's coefficients. Typical values selected for theoretical calculations are given in Table I [6].

Table I. Optical fiber constants used in calculations

α_s	Substrate coefficient of thermal expansion	13.1 x 10^{-6} /°C
α_f	Fiber coefficient of thermal expansion	0.55 x 10^{-6} /°C
n_0	Refraction index	1.46
dn_0/dT	Thermo-optic coefficient	11 x 10^{-6} /°C
ν	Poisson ratio	0.2
p_{11}, p_{12}	Pockel's coefficients	0.113, 0.252

The mechanical strain can be calculated two different ways. The strain of the fiber surface is equivalent to the applied strain from the substrate in case of good contact and can be approximated by the following simple "CTE" equation:

$$\varepsilon = \alpha_s \left(T - T_0\right) \tag{9}$$

where α_s is the coefficient of thermal expansion of the substrate. Alternatively, the mechanical strain can be calculated via the analysis of a bimetallic beam. When a beam made up of two strips of materials of different elastic moduli and of different coefficients of thermal expansion is subject to a uniform temperature change it will bend [11]. Its curvature and deflection, as well as the mechanical strain in the axial direction of either of the two strips, can be calculated. The curvature of a bimetallic beam is not very sensitive to differences in elastic moduli but is rather sensitive to the differences in the coefficients of thermal expansion [11]. Using this assumption it can be shown that the mechanical strain in the axial direction in the top strip can be calculated using the following "beam" equation:

$$\varepsilon = \alpha_{top}\left(T - T_0\right) + \frac{1}{4}\frac{\left(\alpha_{bottom} - \alpha_{top}\right)}{\left(1 + \frac{E_{top}}{E_{bottom}}\right)}\left(T - T_0\right) - \frac{3}{2h}\left(\alpha_{bottom} - \alpha_{top}\right)\left(y - \frac{h}{4}\right)\left(T - T_0\right) \tag{10}$$

where y is measured from the bottom of the bottom strip, h is the total thickness of both strips, α_{top} is the coefficient of thermal expansion (CTE) of the top strip, α_{bottom} is the coefficient of thermal expansion (CTE) of the bottom strip, E_{top} is the elastic modulus of the top strip, and E_{bottom} is the elastic modulus of the bottom strip. In our case the top strip is nickel and the bottom strip is copper. This analysis can be applied to calculate the mechanical strain in the nickel coating layer of our nickel plated copper substrate near the embedded FBG sensor. The effects of mechanical strain not in the axial direction have been ignored.

The temperature measured by the FBG sensor can be predicted with the following equation:

$$T = \frac{1}{m}\left(\lambda - \lambda_0\right) + T_0 \tag{11}$$

where m is the sensitivity (either theoretical or experimental), λ is the Bragg wavelength, and λ_0 and T_0 are the Bragg wavelength and temperature measured at calibration, respectively.

Results

To test the accuracy of the thermal response, the nickel-coated copper substrate containing the embedded FBG sensor and the free-floating FBG sensor was heated with a heat gun, and allowed to cool. Further tests were conducted by cooling in ice water. Signals from the FBG sensors were recorded using an O/E Land interrogator and software. For validation, a Type K thermocouple was silver pasted to the surface of the nickel above the embedded FBG sensor to record the actual temperature. The temperature measured by the thermocouple is plotted against the wavelength signal of the FBG sensors in Fig. 5. The two FBG sensors exhibit different sensitivities, or slopes. Computing the slopes of the two sets of experimental points gives the following measured sensitivities: 0.0294 nm/°C for the sensitivity of the nickel embedded FBG sensor with a Bragg wavelength of 1543.30 nm and 0.0122 nm/°C for the free-floating FBG sensor with a Bragg wavelength of 1541.04 nm. The nickel coating increases the sensitivity of the FBG sensor by more than twice due to its high coefficient of thermal expansion that imposes significant strain, stretching the fiber more as temperature increases.

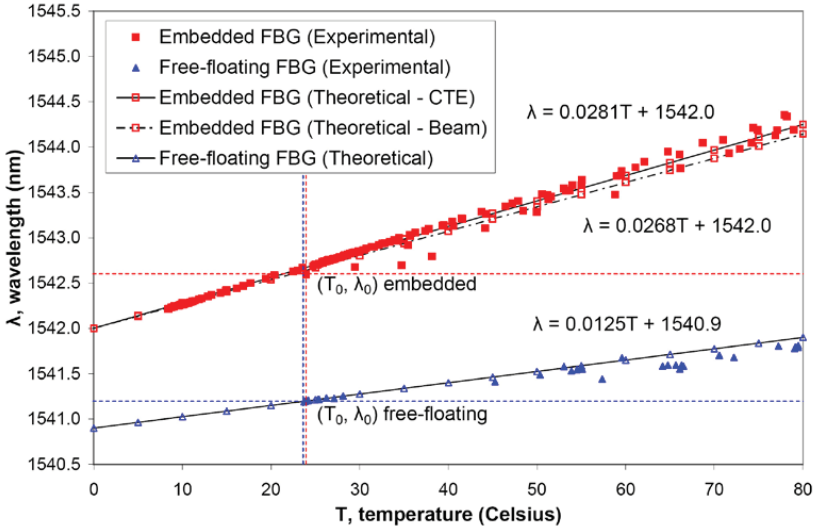

Figure 5. Thermal response of embedded and free-floating FBG sensors (intersection of dashed lines indicates start of experiment/calibration point).

Notice that several temperature measurements near the calibration point corresponding to the first heating of the embedded FBG sensor do not follow the theoretical prediction. This was not observed as the FBG sensor and assembly was allowed to cool back to room temperature, or during subsequent cycles. It is hypothesized that the polyimide coating allowed the cladding and core to "slip" within the coating during the first 10 or 20°C increase from room temperature during the first heating. For all subsequent heating and cooling cycles, it appears that a strong bond developed between the fiber and the substrate.

The theoretical sensitivity for the free-floating FBG sensor was calculated as 0.0125 nm/°C using Eqn. 5 with mechanical strain calculated using Eqn. 9 with α_f substituted for α_s. This means that no mechanical force acts upon the free-floating FBG sensor. This calculation shows that the experimental sensitivity is 2.1% off from the theoretical sensitivity for the free-floating FBG sensor. The theoretical sensitivity for the embedded FBG sensor was calculated as 0.0281 nm/°C using Eqn. 9 to compute the mechanical strain (CTE method), shown plotted on the above

figure. The alternative method of calculating mechanical strain using Eqn. 10 (beam method), produces a theoretical sensitivity for the embedded FBG sensor of 0.0268 nm/°C, shown plotted on the above figure. Both methods of predicting the mechanical strain yield theoretical sensitivities approximately 5% off the experimental sensitivity. When using Eqn. 10, this error is most likely due to the fact that the temperature change applied during testing is most likely not uniform.

To avoid calibration, the free-floating FBG sensor gives correct absolute temperature predictions for the reference temperature, $T_0^{'}$, of 10°C, (which is presumably the actual ambient temperature that corresponds with the center wavelength, λ_{CW}, from the manufacturer). For the embedded fiber, the reference temperature $T_0^{'}$ appears to be 48°C. This is presumably higher than the actual reference temperature from manufacturing. This is likely due to mechanical strain due to compressive residual stress arising during the electro-plating process. Assuming the same actual reference temperature of 10°C, and an elastic modulus of 207 GPa for the nickel coating layer, this corresponds to a residual stress, $\sigma = -E\alpha_s\left(T - T_0^{'}\right)$, of -103 MPa. This result makes sense, although it is not obvious. Often coating layers are manufactured in compression, as the mold at steady-state goes into tension. With the residual compression, adding the tension will produce a net stress that is hopefully still in compression, thus causing fatigue cycles that are entirely in compression, and thus not a problem. Fatigue cycles involving tension would surely cause plating cracks quickly, given the high level of tensile stress calculated in the next section. If the tension can overcome the initial compressive stress in the coating layer, then cracks in the coating layer might develop. This might happen over time, owing to high-temperature creep. The embedded sensor would provide a lifetime measurement of this stress

Conclusions

A new method to measure temperature and/or heat flux near the surface of the hot face of continuous casting molds has been designed. It consists of embedding a thin optical fiber with fiber Bragg gratings inside a thin stainless steel tube into the nickel coating layer during electrodeposition onto the surface of the copper molds used to continuous cast steel slabs and/or billets. During casting, this sensor will monitor the thermal condition of the mold. The sensors inside the fiber function using optical-based technology (resonating frequency of light captured in an embedded optical fiber system causes the wavelength of light emitted along the fiber to depend on thermal strain, which varies with the temperature).

Embedded sensors have the advantage of real-time monitoring at critical locations as well as immunity to electromagnetic interference and resistance to hostile environments, but cannot be commercial successful without a robust attachment method. Key advantages of the new sensor over conventional thermocouples include:

- The small size of the active sensor is much smaller than current thermocouple beads, allowing greater sensitivity to temperature variations both spatially and temporally;
- The active part of the sensor is embedded inside a fiber, and protected by a metal tube, allowing it to be manufactured in a controlled environment, and handled, prior to attaching to the dirty environment of the mold;
- The attachment method of embedding into the coating layer during the electroplating process allows the sensor to be close to (but not at) the mold surface without drilling a hole through the mold or otherwise damaging its structural integrity.

- The proximity of less than 1 mm from the mold surface is more than an order of magnitude closer to the hot face surface than conventional thermocouples, giving corresponding better resolution of thermal and strain events.

The new sensor can provide new insight into transient temperature and heat flux behavior of casting molds. It solves several problems inherent to conventional thermocouple systems (currently used to monitor mold wall temperature), and conventional mold level sensors (currently used to monitor mold level). If a second optical fiber is embedded, then the sensor can additionally monitor thermal stresses in the mold surface, enabling it to provide feedback to signal crack formation in the coating layer.

Acknowledgements

Funding for this work was provided by the National Science Foundation (Grant CMMI 05-28668) and the Continuous Casting Consortium at the University of Illinois. Optical microscopy was carried out in the Frederick Seitz Materials Research Laboratory Central Facilities, University of Illinois, which is partially supported by the U.S. Department of Energy under grants DE-FG02-07ER46453 and DE-FG02-07ER46471. Special thanks are extended to Mike Powers of Siemens VAI Services, LCC for assistance with trials.

References

1. R. Caskey, “Thermal Mold Level Control at Nucor Steel Seattle Inc.”, AISTech 2008, Steelmaking Conference Proc., Pittsburgh, PA, May 5-8, 2008, Assoc. Iron Steel Tech., Warrendale, PA, Vol. 1, 2008.
2. W. H. Emling and S. Dawson: 'Mold Instrumentation for Breakout Detection and Control', 74th Steelmaking Conf., Washington, D.C., 14-17, Apr., 1991, ISS, Warrendale, PA, 197-217.
3. B. G. Thomas: 'On-line Detection of Quality Problems in Continuous Casting of Steel', in 'Modeling, Control and Optimization in Ferrous and Nonferrous Industry', (eds. F. Kongoli, et al.), 29-45; 2003, TMS, Warrendale, PA, 2003.
4. A. B. Badri and A. W. Cramb: 'Heat Flux Calculation from Thermocouples-What can be measured?', 85th Steelmaking Conf., Nashville, TN, Mar. 10-13, 2002, ISS Society, 65-76.
5. B.G. Thomas, M.A. Wells, and D. Li, “Monitoring of Meniscus Thermal Phenomena with Thermocouples in Continuous Casting of Steel”, in “Sensors, Sampling, and Simulation for Process Control”, TMS Annual Meeting, San Diego, CA, 2010.
6. M. Okelman, “Design and Installation of Novel Sensors into the Continuous Casting Mold”, MS Thesis, University of Illinois, 2008.
7. Udd, E., Fiber Optic Smart Structures. 1995, New York: Wiley (Interscience).
8. M. K. Okelman, B. G. Thomas, and M. Powers: 'Effect of geometry on void formation in commercial electroplating of thin strips to copper', Surface & Coatings Technology, 2008, 202(17), 4153-4158.
9. Sirkis, J.S. and A. Dasgupta, What Do Embedded Optical Fibers Really Measure?, in 1st European Conference on Smart Structures and Materials. 1992, EOS/SPIE and IOP Publishing: Glasgow. p. 69-72.
10. Li, X. and F. Prinz, Metal Embedded Fiber Bragg Grating Sensors in Layered Manufacturing. Journal of Manufacturing Science and Engineering, 2003. 125: p. 1-9.
11. Timoshenko, S., Bending and Buckling of Bimetallic Strips. J. Optical Soc. of Am., 1925. 11: p. 233.